

**Polarimetric Signatures of Moving Automotive Vehicles Based on H/A/ α -decomposition
Preliminary Results with PARSAX Radar Data**

Bosma, Detmer A.; Krasnov, Oleg A.; Yarovoy, Alexander

Publication date

2022

Document Version

Final published version

Published in

Proceedings of the 2022 23rd International Radar Symposium (IRS)

Citation (APA)

Bosma, D. A., Krasnov, O. A., & Yarovoy, A. (2022). Polarimetric Signatures of Moving Automotive Vehicles Based on H/A/ α -decomposition: Preliminary Results with PARSAX Radar Data. In *Proceedings of the 2022 23rd International Radar Symposium (IRS)* (pp. 414-419). IEEE.
<https://ieeexplore.ieee.org/document/9905019>

Important note

To cite this publication, please use the final published version (if applicable).
Please check the document version above.

Copyright

Other than for strictly personal use, it is not permitted to download, forward or distribute the text or part of it, without the consent of the author(s) and/or copyright holder(s), unless the work is under an open content license such as Creative Commons.

Takedown policy

Please contact us and provide details if you believe this document breaches copyrights.
We will remove access to the work immediately and investigate your claim.

Green Open Access added to TU Delft Institutional Repository

'You share, we take care!' - Taverne project

<https://www.openaccess.nl/en/you-share-we-take-care>

Otherwise as indicated in the copyright section: the publisher is the copyright holder of this work and the author uses the Dutch legislation to make this work public.

Polarimetric Signatures of Moving Automotive Vehicles Based on $H/A/\alpha$ -decomposition: Preliminary Results with PARSAX Radar Data

Detmer A. Bosma

Microwave Sensing, Signals & Systems
Delft University of Technology
Delft, the Netherlands
D.A.Bosma@tudelft.nl

Oleg A. Krasnov

Microwave Sensing, Signals & Systems
Delft University of Technology
Delft, the Netherlands
O.A.Krasnov@tudelft.nl

Alexander Yarovoy

Microwave Sensing, Signals & Systems
Delft University of Technology
Delft, the Netherlands
A.Yarovoy@tudelft.nl

Abstract—Polarimetric radar responses from moving automotive targets are studied aiming at target classification using the polarimetric $H/A/\alpha$ -decomposition technique. A signal- and data processing chain has been proposed for the detection and tracking of targets in a multi-target environment in the range-Doppler domain. Polarimetric information of the vehicles is collected during tracking and is analyzed by the $H/A/\alpha$ -decomposition technique. Employing both time averaging and spatial averaging of the statistical coherency matrix, the polarimetric signatures of both vehicles and static clutter have been presented in the two-dimensional H/α -plane. It has been found that the spatial averaging approach results in a polarimetric signature that can be very helpful to distinguish automotive vehicles from static clutter.

Index Terms—polarimetric radar, polarimetric signature, $H/A/\alpha$ -decomposition, polarimetric fusion, target detection, multi-target tracking

I. INTRODUCTION

Nowadays, many practical radar applications require an automatic interpretation of the received data, including data processing algorithms for automatic tracking and classification of objects of interest observed by the radar, also called targets. To this end, the availability of labeled data sets and information about the characteristics of the target, also known as its signature, is crucial.

In this research, we aim for advancing the state-of-the-art in automatic target detection, tracking, and classification by exploiting modern polarimetric waveforms. These waveforms facilitate the ability to measure all four elements of the *polarization scattering matrix* (PSM) simultaneously. These elements (HH, HV, VH & VV) consist of complex data, meaning that both amplitude and phase information of the received signals are provided [1]. Radars capable of measuring these polarimetric characteristics of targets provide valuable additional information for more reliable target detection, more accurate target identification, and better parameter estimation. The exploitation of polarimetric-Doppler characteristics is a very promising concept to improve automotive vehicle classification and can be applied in both automotive radar and

surveillance radar applications, such as road traffic control and monitoring [2] or feature-aided tracking of vehicles [3].

The four components of the PSM can be decomposed for an easier physical interpretation [4] and can therefore be used to describe the polarimetric signatures of certain classes of objects. Besides the commonly-used, coherent decomposition techniques, such as the Pauli and Krogager decomposition, the $H/A/\alpha$ -decomposition is a typical and useful method to describe the target scattering mechanism [5].

The goal of this research is to define the polarimetric signature of moving automotive vehicles based on the polarimetric $H/A/\alpha$ -decomposition technique. In order to apply this decomposition technique, all moving vehicles that can be observed by the four polarization channels of the polarimetric radar, need to be detected and tracked over time, which is most straightforwardly performed in the range-Doppler domain. A dedicated signal and data processing chain to process the real-world data, gathered by the fully polarimetric-Doppler surveillance S-band radar PARSAX (see [1], [6], [7]), established by the TU Delft and originally designed as weather radar, has been developed. After a polarimetric data fusion algorithm has been applied, target detection is performed.

Subsequently, a multi-target tracking algorithm is implemented to track each vehicle over time. During this process, polarization information of the clusters corresponding to the moving vehicles is collected and used to describe the polarization scattering characteristics of these targets using the $H/A/\alpha$ -decomposition.

The remaining part of the paper is structured as follows: in Section II the signal and data processing chain is presented and the $H/A/\alpha$ -decomposition technique is explained. Moreover, in Section III the results of the research are discussed. At last, the conclusions and recommendations for future research are presented in Section IV.

II. SIGNAL AND DATA PROCESSING CHAIN

The main idea of this decomposition technique is that the H , A , and α features of the targets can be used to identify the underlying average scattering mechanism. These parameters

are extracted from an eigenvalue analysis of the average coherency matrix \mathbf{T} [8], which can be derived by either time averaging or spatial averaging. Hence, it is required to find clusters of detected cells that represent the targets and to track each target over time. Therefore, all moving vehicles that can be observed by the radar, need to be detected and tracked, which is most straightforwardly performed in the range-Doppler domain.

As a result, a dedicated signal and data processing chain to process the real-world data, originating from the fully polarimetric-Doppler S-band FMCW surveillance radar PARSAX, has been developed, as illustrated in Fig. 1.

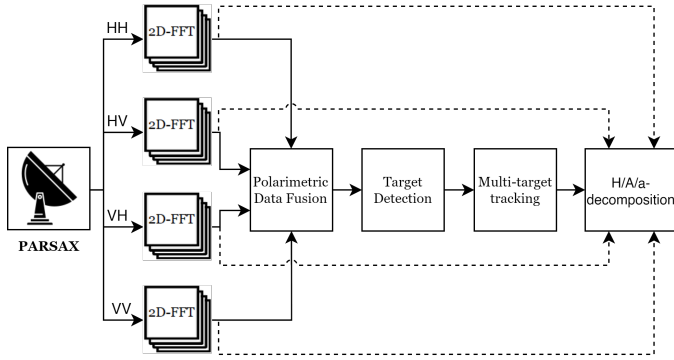


Fig. 1. Signal and data processing chain for the four polarization channels before the $H/A/\alpha$ -decomposition is performed

A. Doppler processing

As target detection will be applied in the range-Doppler domain, a two-dimensional FFT is performed over fast and slow time to provide the range-Doppler map for each of the four polarimetric channels. Beforehand, the sampled IF radar signals are pre-processed and a *high-pass filter* (HPF) is applied to remove static clutter [9]. After the Doppler processing steps of 512 pulses per time frame, the strong reflections of the moving vehicles can clearly be seen in the range-Doppler map, as shown in Fig. 2. Here the Doppler frequency is converted to the radial velocity.

B. Polarimetric data fusion

Before target detection takes place, to gain full advantage of the additional polarimetric information, all four data sets are exploited by a data fusion method to improve the detection performance. All four range-Doppler spectra, corresponding to the four elements of the PSM, are integrated into a single range-Doppler map per time frame.

By comparing several polarimetric fusion methods, Novak *et al.* [10] have shown that the *Polarimetric Maximization Synthesis Detector* (PMSD) exhibits the highest detection performance without any a priori information about the polarization characteristics of the targets and/or clutter. Therefore, a fusion method based on the PMSD has been implemented.

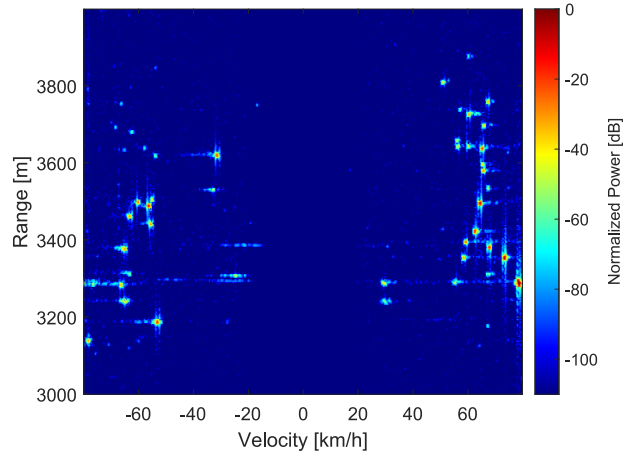


Fig. 2. A range-Doppler map of real-world data, representing a dense highway, visualizing only moving vehicles. This map originates from the HH-channel, the other polarization channels (HV, VH & VV) show similar results.

C. Target detection in range-Doppler domain

Target detection means deciding for each range-Doppler bin whether a target is present or not. Often this decision is based on a threshold with respect to the amplitude/power measurement of the range-Doppler bin. This threshold can either be a fixed, non-adaptive amplitude value or an adaptive threshold based on the estimation of the local noise level, which is incorporated in the commonly-used *Constant False Alarm Rate* (CFAR) detector. To detect the moving vehicles in the range-Doppler domain, the *Ordered Statistics* (OS) CFAR detector is selected over the non-adaptive detector and other CFAR detector variants, since the OS-CFAR is more robust to noise fluctuations and shows a higher detection performance in a dense target environment [9], such as a highway.

Imperfections and distortions (due to noise, clutter, and other limitations) of the resulted binary detection map are resolved by applying a morphological filter [11], exploiting the aliasing property of Doppler processing, and discarding detections with low velocity by an additional HPF. Subsequently, the DBSCAN clustering algorithm is applied such that a group of detected cells represent a single target [12], which will simplify the tracking algorithm significantly.

As input for the OS-CFAR detector, the probability of false alarm P_{FA} is set to 10^{-8} , the number of guard cells N_g to [6, 4] and the number of training cells N_t to [6, 6]. An example of the resulted target detection and clustering performance can be seen in Fig. 3.

D. Multi-target tracking

In order to track multiple targets from frame to frame, a *multi-target tracking* (MTT) algorithm is developed. The block diagram of a basic MTT algorithm is shown in Fig. 4.

The state of the i^{th} target at the k^{th} time frame \mathbf{x}_k^i is described by its true range and true velocity. Based on the clusters found in the detection map of the fused range-Doppler frame, each target i is represented by a single noisy

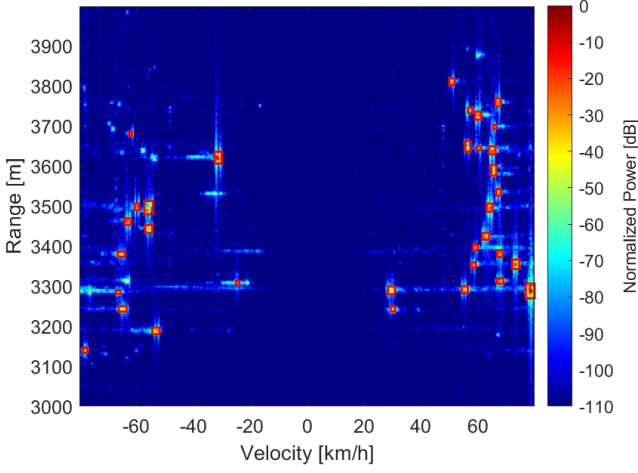


Fig. 3. Resulted detection map and clusters (indicated by red boxes) after applying polarimetric data fusion and the OS-CFAR detector

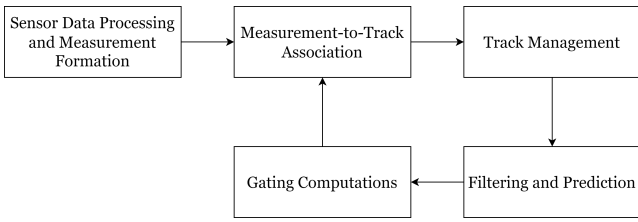


Fig. 4. A block diagram of the basic elements of a MTT-algorithm [13]

measurement \mathbf{z}_k^i at time frame k . Each measurement can be described by the observed states, which include a range value R and a velocity value v and are selected by the state observation matrix \mathbf{H} , following

$$\mathbf{z}_k^i = \mathbf{H}\mathbf{x}_k^i + \mathbf{v}_n, \quad (1)$$

where $\mathbf{v}_n \sim \mathcal{N}(0, \Sigma_n)$ represents zero-mean Gaussian measurement noise with the noise variances $\sigma_{n,R}^2$ and $\sigma_{n,v}^2$ on the diagonal of Σ_n .

A classical Kalman filter is used to update and predict the state of each target following the constant acceleration (CA) state dynamics model. This model is selected based on its accurate approximation of the behavior of moving vehicles on a highway and is well-suited for tracking purposes in the range-Doppler domain. With this model, each state can be described by the target's range, velocity, and acceleration. This provides the following state transition model matrix \mathbf{F} , state observation matrix \mathbf{H} , and process noise covariance matrix \mathbf{W} :

$$\mathbf{F} = \begin{bmatrix} 1 & T & T^2/2 \\ 0 & 1 & T \\ 0 & 0 & 1 \end{bmatrix}, \quad (2a)$$

$$\mathbf{H} = \begin{bmatrix} 1 & 0 & 0 \\ 0 & 1 & 0 \end{bmatrix}, \quad (2b)$$

$$\mathbf{W} = \begin{bmatrix} T^4/4 & T^3/2 & T^2/2 \\ T^3/2 & T^2 & T \\ T^2 & T & 1 \end{bmatrix}, \quad (2c)$$

where T is the time step between successive range-Doppler frames.

First, the target's predicted state $\hat{\mathbf{x}}_{k|k-1}$ will be estimated based on its previous state $\hat{\mathbf{x}}_{k-1|k-1}$. Besides, the predicted state covariance matrix $\hat{\mathbf{Q}}_{k|k-1}$ is computed based on its previous state covariance matrix $\hat{\mathbf{Q}}_{k-1|k-1}$ and the process noise covariance matrix \mathbf{W} . This is described by

$$\hat{\mathbf{x}}_{k|k-1} = \mathbf{F}\hat{\mathbf{x}}_{k-1|k-1}, \quad (3a)$$

$$\hat{\mathbf{Q}}_{k|k-1} = \mathbf{F}\hat{\mathbf{Q}}_{k-1|k-1}\mathbf{F}^T + \sigma_w^2\mathbf{W}, \quad (3b)$$

where σ_w^2 is the process noise variance. Subsequently, based on the gain \mathbf{K}_k , computed by the predicted covariance matrix $\hat{\mathbf{Q}}_{k|k-1}$, the target's current state $\hat{\mathbf{x}}_{k|k}$ and the target's current state covariance matrix $\hat{\mathbf{Q}}_{k|k}$ will be estimated as follows:

$$\mathbf{K}_k = \hat{\mathbf{Q}}_{k|k-1}\mathbf{H}^T (\mathbf{H}\hat{\mathbf{Q}}_{k|k-1}\mathbf{H}^T + \Sigma_n)^{-1}, \quad (4a)$$

$$\hat{\mathbf{x}}_{k|k} = \hat{\mathbf{x}}_{k|k-1} + \mathbf{K}_k (\mathbf{z}_k - \mathbf{H}\hat{\mathbf{x}}_{k|k-1}), \quad (4b)$$

$$\hat{\mathbf{Q}}_{k|k} = (\mathbf{I} - \mathbf{K}_k\mathbf{H})\hat{\mathbf{Q}}_{k|k-1}, \quad (4c)$$

where \mathbf{I} is a 3×3 identity matrix [13].

To associate each measurement to a certain target, the *Global Nearest Neighbor* (GNN) method, based on minimizing the total distance, has been implemented. Beforehand, to simplify the data association problem, a hyperellipsoid gate, which incorporates the statistical Mahalanobis distance, is applied [9]. To cope with Doppler ambiguity, a *Multiple Hypothesis Tracking* (MHT) based solution has been proposed, based on the work of Li *et al.* [14]. The hypothesis with the highest probability will determine whether the track can consider the velocity measurement to be folded or not. At last, an M/N logic test is selected to solve the track management problem, such that all unassigned measurements will initialize a new track, and all tracks that are not associated with a measurement will be canceled [15].

E. $H/A/\alpha$ -decomposition

While tracking all moving targets, the amplitude and phase information of all four polarization channels will be collected. This polarimetric information can be applied to polarimetric decomposition techniques, which can provide more information and a better insight into the physical meaning of the scattering of the moving vehicles [16]. Under the assumption of the monostatic back-scattering case, the reciprocity rule applies (i.e., $S_{HV} = S_{VH}$). Therefore, to characterize the target scattering, the PSM of each range-Doppler bin can be represented by the Pauli scattering vector $\tilde{\mathbf{k}}_P$, described by

$$\tilde{\mathbf{k}}_P = \frac{1}{\sqrt{2}} \begin{bmatrix} S_{HH} + S_{VV} \\ S_{HH} - S_{VV} \\ S_{HV} + S_{VH} \end{bmatrix} \quad (5)$$

where $[\cdot]^T$ denotes a transpose operation. The average coherency matrix \mathbf{T} , based on the statistical average of all the scattering information, is then defined by

$$\mathbf{T} = \langle \tilde{\mathbf{k}}_P \cdot \tilde{\mathbf{k}}_P^H \rangle, \quad (6)$$

where $[\cdot]^H$ denotes the conjugate transpose operation. As these decomposition techniques aim to provide an interpretation of the scattering mechanism, it is assumed that the average target scattering is invariant to polarization changes. Therefore, averaging can be performed in any domain (e.g., time domain, spatial domain, angular domain).

Within the $H/A/\alpha$ -decomposition method, the polarimetric entropy H is a quantitative measure of randomness in the scattering mechanisms, the anisotropy A is used to characterize the scattering phenomenon, and the alpha angle ($0^\circ \leq \alpha \leq 90^\circ$) represents the surface scattering characteristics from isotropic surface scattering to dipole scattering to dielectric dihedral scattering [8], [16]. These parameters can be very useful to characterize the scattering properties [5].

To compute these parameters, the average coherency matrix \mathbf{T} is decomposed as

$$\mathbf{T} = \mathbf{U}\mathbf{\Lambda}\mathbf{U}^H = \mathbf{U} \begin{bmatrix} \lambda_1 & 0 & 0 \\ 0 & \lambda_2 & 0 \\ 0 & 0 & \lambda_3 \end{bmatrix} \mathbf{U}^H, \quad (7)$$

where \mathbf{U} is a unitary matrix containing three orthogonal eigenvectors \mathbf{u}_i , and $\mathbf{\Lambda}$ is a 3×3 diagonal matrix with non-negative real eigenvalues ($\lambda_1 \geq \lambda_2 \geq \lambda_3 \geq 0$). If all eigenvalues λ_i are zero, except for λ_1 , then the coherency matrix \mathbf{T} represents a single scattering matrix, corresponding to a pure correlated and completely polarized scattering mechanism. On the other hand, if all eigenvalues are identical, then \mathbf{T} corresponds to a completely unpolarized, random scattering process [5]. To define the polarimetric entropy H and alpha angle α , the pseudo-probabilities P_i need to be obtained from the eigenvalues λ_i ($i = 1, 2, 3$), which can be described as follows:

$$P_i = \frac{\lambda_i}{\sum_{j=1}^3 \lambda_j}. \quad (8)$$

The $H/A/\alpha$ -decomposition is then defined by

$$H = - \sum_{i=1}^3 P_i \log_3(P_i), \quad (9a)$$

$$A = \frac{\lambda_2 - \lambda_3}{\lambda_2 + \lambda_3}, \quad (9b)$$

$$\alpha = \sum_{i=1}^3 P_i \cos^{-1}(|u_{i,1}|), \quad (9c)$$

where $u_{i,1}$ is first element on the eigenvector \mathbf{u}_i [8]. These equations show that the polarimetric entropy is $H = 0$ for a completely deterministic and $H = 1$ for a completely random scattering mechanism. A completely deterministic scattering mechanism, meaning that the scattering wave is completely polarized, results in a degree of polarization of 1. Correspondingly, completely random scattering (i.e., $H = 1$) leads to a degree of polarization of 0. In the latter case, the process is completely depolarizing and polarimetric information is useless for classification [5].

Since the anisotropy A only becomes an important and useful parameter to describe the scattering process when the

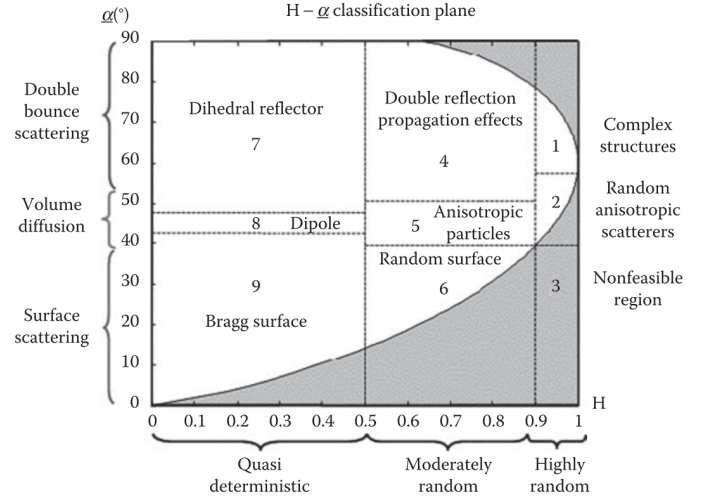


Fig. 5. Simple classification scheme of the two-dimensional H/α -plane [5]

entropy H is very high, classification is often performed in the two-dimensional H/α -plane. This H/α -plane can be separated into 9 classes of basic scattering mechanisms, as presented in Fig. 5. This figure illustrates a simple schematic overview to classify and describe the scattering mechanism based on typical values of the entropy H and α angle [5], [8].

III. RESULTS

The proposed signal and data processing chain (see Fig. 1) has been applied to real-world polarimetric radar data, captured by the PARSAX radar, while observing a dense highway (A13, between Delft and Rotterdam). As a result, polarimetric information of 66 targets in a time period of 46.5 s, representing 93 time frames, has been acquired.

The $H/A/\alpha$ -decomposition technique has been utilized to describe the polarimetric signature of the moving automotive vehicles. To characterize the scattering of the vehicles, the average coherency matrix \mathbf{T} needs to be defined for each target. Therefore, averaging is required (see (6)), which for this application can either be time averaging or spatial averaging. Besides, to compare the characteristics of the targets, polarimetric information of static clutter, which had been filtered out during pre-processing, has been collected as well.

A. Time averaging

In order to perform time averaging to get the average coherency matrix \mathbf{T}_{time} , the PSM of the target's centroid bin of each time frame is collected and averaged over time, resulting in a single value for H , A and α for each target. A two-dimensional histogram of the entropy H and α angle of 66 targets has been visualized in the H/α -plane, as shown in Fig. 6.

As can be seen, the entropy is distributed in the region $0.3 \leq H_{time} \leq 0.8$ and around $\alpha_{time} \approx 45^\circ$. According to the classification schematic in Fig. 5, this is correlated to volume diffusion and quasi-deterministic/moderately random entropy, corresponding to dipole and anisotropic particle scattering.

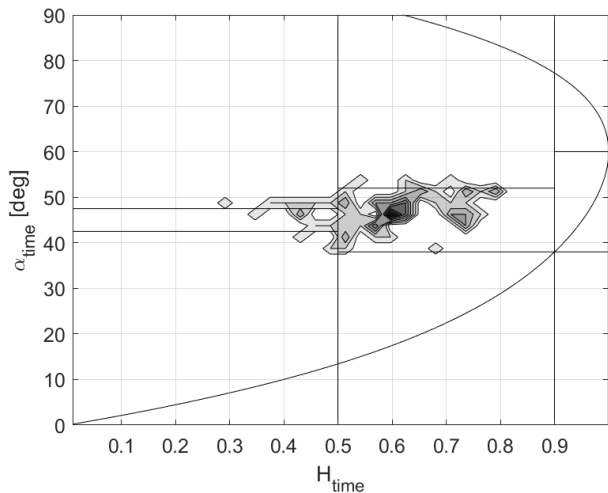


Fig. 6. Two-dimensional histogram in the H/α -plane of moving automotive vehicles, based on time averaging of the coherency matrix \mathbf{T}_{time}

Since only the centroid is taken into account, this is probably related to the scattering of the main body of a vehicle.

This time averaging approach has been performed with the polarimetric information of the static clutter as well. This results in the two-dimensional histogram in the H/α -plane in Fig. 7, which shows many similarities with the histogram corresponding to moving vehicles. Hence, this approach is not considered useful to describe the polarimetric signature of moving automotive vehicles.

B. Spatial averaging

Spatial averaging is implemented to get the average coherency matrix \mathbf{T}_{space} . In this case, the PSM of all bins of each target's cluster is collected and averaged, resulting in a single value for H , A , and α for each target for each time frame. This results in 93 values for H , A and α per target.

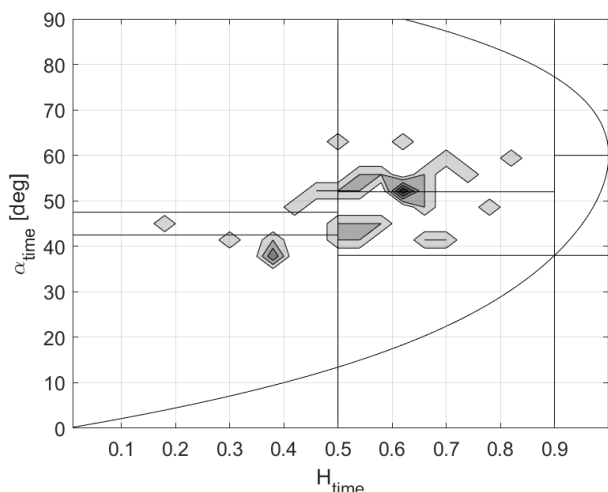


Fig. 7. Two-dimensional histogram in the H/α -plane of static clutter, based on time averaging of the coherency matrix \mathbf{T}_{time}

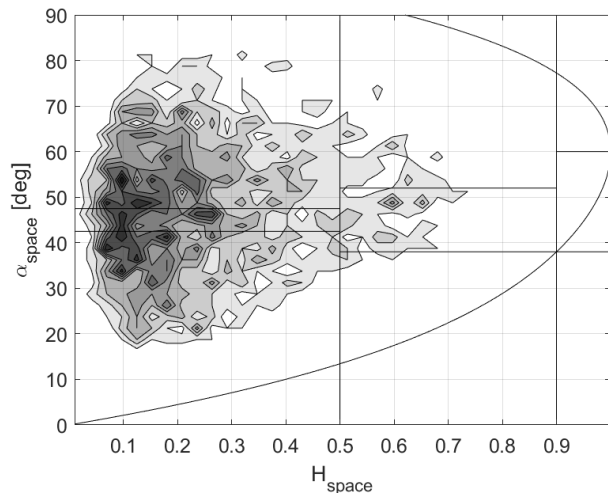


Fig. 8. Two-dimensional histogram in the H/α -plane of moving automotive vehicles, based on spatial averaging of the coherency matrix \mathbf{T}_{space}

Again, the two-dimensional histogram of all targets of all time frames has been visualized in the H/α -plane in Fig. 8.

As can be seen, a high concentration in the region at $H_{space} \leq 0.3$ and $30^\circ \leq \alpha_{space} \leq 70^\circ$ is present, corresponding to quasi-deterministic entropy with all kinds of scattering mechanisms. Since the target's cluster covers reflections from all parts of the vehicle (i.e., the main body, the wheels, car mirrors, etc.), there is an obvious explanation for this scattering behavior in the H/α -plane.

Similarly, spatial averaging has been applied to the polarimetric information of the static clutter as well. The resulted distribution in Fig. 9 shows that there is a big difference in the scattering properties with respect to moving vehicles. Therefore, this averaging approach is very suitable to describe the polarimetric signature of moving vehicles and can be very helpful to distinguish these vehicles from static clutter, even when velocity information is not available.

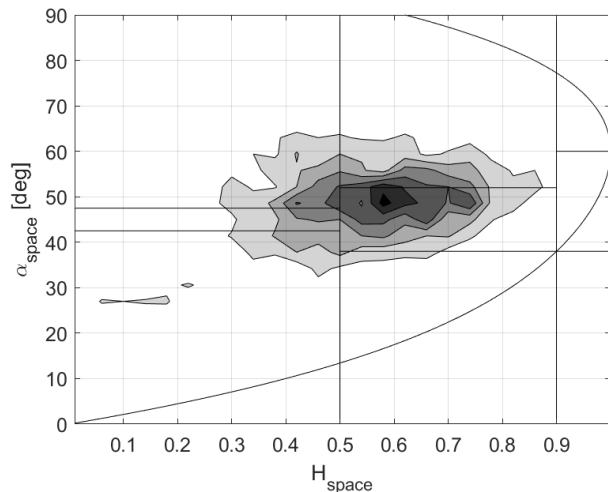


Fig. 9. Two-dimensional histogram in the H/α -plane of static clutter, based on spatial averaging of the coherency matrix \mathbf{T}_{space}

IV. CONCLUSION AND FUTURE RESEARCH

A dedicated signal and data processing chain has been developed to detect and track the targets in a multi-target environment in the range-Doppler domain, exploiting polarimetric data fusion, the OS-CFAR detector, and a multi-target tracking algorithm. The $H/A/\alpha$ -decomposition technique has been introduced and has been applied to real-world polarimetric radar data, captured by the fully polarimetric S-band PARSAX radar, representing the scattering from a highway with dense traffic. The entropy H , anisotropy A , and α angle are used to describe scattering characteristics and are computed by the average coherency matrix \mathbf{T} . Employing both time averaging and spatial averaging, the characteristics of both the targets and static clutter have been visualized by two-dimensional histograms in the H/α -plane. It has been shown that the spatial averaging approach is very suitable to describe the polarimetric signature of moving automotive vehicles.

As these results are based on only 66 targets and only a narrow sector of the aspect angle, in the future larger data sets of multiple aspect angles of the vehicles will be analyzed. Moreover, the effect of applying these signatures on the classification performance of moving vehicles should be analyzed by implementing a classifier.

ACKNOWLEDGMENT

The authors would also like to thank Fred van der Zwan for his assistance with the measurements.

REFERENCES

- [1] O. A. Krasnov and L. P. Ligthart, "Radar polarimetry using sounding signals with dual orthogonality - PARSAX approach," in *European Microwave Week (EuMW) - 7th European Radar Conference (EuRAD) 2010*. Paris, France: IEEE, 2010, pp. 121–124.
- [2] G. Wanielik, N. Appenrodt, H. Neef, R. Schneider, and J. Wenger, "Polarimetric millimeter wave imaging radar and traffic scene interpretation," in *IEE Colloquium on Automotive Radar and Navigation Techniques (Ref. No. 1998/230)*. IET, 2 1998, pp. 1–4.
- [3] D. H. Nguyen, J. H. Kay, B. J. Orchard, and R. H. Whiting, "Feature-aided tracking of moving ground vehicles," *Algorithms for Synthetic Aperture Radar Imagery IX*, vol. 4727, pp. 234–245, 8 2002.
- [4] S. R. Cloude and E. Pottier, "A review of target decomposition theorems in radar polarimetry," *IEEE Transactions on Geoscience and Remote Sensing*, vol. 34, no. 2, pp. 498–518, 3 1996.
- [5] J. S. Lee and E. Pottier, *Polarimetric radar imaging - from basics to applications*, 1st ed. Boca Raton, FL, USA: CRC Press LLC, 2009.
- [6] O. A. Krasnov, L. P. Ligthart, Z. Li, G. P. Babur, Z. Wang, and F. van der Zwan, "PARSAX: High-resolution Doppler-polarimetric FMCW radar with dual-orthogonal signals," in *4th Microwave and Radar Week - 18th International Conference on Microwaves, Radar and Wireless Communications 2010*. Vilnius, Lithuania: IEEE, 2010, pp. 1–5.
- [7] S. Neemat, O. A. Krasnov, E. Goossens, and A. Yarovoy, "Radar polarimetry with interleaved dual-orthogonal and time-multiplexed signals: The PARSAX radar setup and preliminary results," in *11th European Conference on Antennas and Propagation (EUCAP) 2017*. Paris, France: IEEE, 3 2017, pp. 3931–3935.
- [8] S. R. Cloude and E. Pottier, "An entropy based classification scheme for land applications of polarimetric SAR," *IEEE Transactions on Geoscience and Remote Sensing*, vol. 35, no. 1, pp. 68–78, 1 1997.
- [9] M. A. Richards, *Fundamentals of radar signal processing*, 2nd ed. McGraw-Hill Education, 2013.
- [10] L. M. Novak, M. B. Seciitin, and M. J. Cardullo, "Studies of target detection algorithms that use polarimetric radar data," *IEEE Transactions on Aerospace and Electronic Systems*, vol. 25, no. 2, pp. 150–165, 3 1989.

- [11] P. Soille, *Morphological image analysis - principles and applications*, 2nd ed. Springer-Verlag Berlin Heidelberg, 2004.
- [12] M. Ester, H.-P. Kriegel, J. Sander, and X. Xu, "A density-based algorithm for discovering clusters in large spatial databases with noise," in *2nd International Conference on Knowledge Discovery and Data Mining*. Portland, OR, USA: AAAI Press, 8 1996, pp. 226–231.
- [13] S. S. Blackman and R. Popoli, *Desing and analysis of modern track systems*. Norwood, MA, USA: Artech House, 1999.
- [14] K. Li, B. Habtemariam, R. Tharmarasa, M. Pelletier, and T. Kirubarjan, "Multitarget tracking with Doppler ambiguity," *IEEE Transactions on Aerospace and Electronic Systems*, vol. 49, no. 4, pp. 2640–2656, 10 2013.
- [15] S. S. Blackman, *Multiple target tracking with radar application*. Norwood, MA, USA: Artech House, 1986.
- [16] T. Visentin, "Polarimetric radar for automotive applications," Ph.D. dissertation, Karlsruhe Institut fur Technologie, 2018.